International Journal of Biological Macromolecules 288 (2025) 138597

Contents lists available at ScienceDirect

International Journal of Biological Macromolecules

journal homepage: www.elsevier.com/locate/ijbiomac

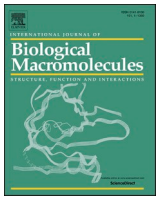

Fabrication and characterization of lactoperoxidase coated the modified graphene oxide-based nanocomposite for medical applications

Abd El Aziz A. Nayl [a,*], Esmail M. El-Fakharany [b,c,d], Ahmed I. Abd-Elhamid [e], Wael A.A. Arafa [a], Ahmed Hamad Alanazi [a], Ismail M. Ahmed [a], Ashraf A. Aly [f], Stefan Bräse [g,**]

[a] Department of Chemistry, College of Science, Jouf University, Sakaka, Aljouf 72341, Saudi Arabia
[b] Protein Research Department, Genetic Engineering and Biotechnology Research Institute GEBRI, City of Scientific Research and Technological Applications (SRTA city), New Borg El-Arab, Alexandria 21934, Egypt
[c] Pharmaceutical and Fermentation Industries Development Centre (PFIDC), City of Scientific Research and Technological Applications (SRTA-City), New Borg El-Arab, Alexandria, Egypt
[d] Pharos University in Alexandria, Canal El Mahmoudia Street, Beside Green Plaza Complex, 21648, Alexandria, Egypt
[e] Composites and Nanostructured Materials Research Department, Advanced Technology and New Materials Research Institute, City of Scientific Research and Technological Applications (SRTA-City), New Borg Al-Arab, Alexandria 21934, Egypt
[f] Chemistry Department, Faculty of Science, Organic Division, Minia University, El-Minia 61519, Egypt
[g] Institute of Biological and Chemical Systems – Functional Molecular Systems (IBCS-FMS), Kaiserstrasse 12, 76131 Karlsruhe, Germany

ARTICLE INFO

Keywords:
Lactoperoxidase nanocombination
Graphene oxide nanocomposite
Copper
Antitumor

ABSTRACT

This study aims to synthesize an innovative (GO-PAA-Cu-LP) nanocomposite through multi-steps for medical applications. First, graphene oxide (GO) was radically anchored with polyacrylic acid (PAA), subsequently, activation through substituting the H-atom of the carboxylic group in PAA with Na-atom. Afterward, Cu-ions are easily loaded over the activated carboxylated groups to act as a satellite in combination with bovine milk lactoperoxidase (LP). The prepared composites were characterized by various techniques, including SEM, TEM, EDX, FTIR, TGA, and XRD analysis, as well as determination of zeta size and potentials for each composite. The experimental results exhibited the ability of LP in the modified form (GO-PAA-Cu-LP) to keep its stability during storage conditions with activity around 73 % of its original reactivity after storage for 9 weeks at 4 °C. The results revealed the selectivity of GO-PAA-Cu-LP against both treated Caco-2 and Huh-7 cells greater than free GO-PAA-Cu composite and free LP. Therefore, these results indicate that the combination of LP with the modified GO-PAA-Cu composite increased its selectivity against all treated cancer cells. These results indicate that the modified GO-PAA-Cu-LP enhanced cell cycle arrest of treated cancer cells in both sub-G1 phase (apoptotic phase) and S phase compared with untreated cells, stimulating apoptotic mechanism.

1. Introduction

Cancer metastasis is one of the most harmful diseases that leads to death in cancer patients. Normally, the doctors require surgery, radiotherapy, and chemotherapy to treat the cancer. These strategies often harm the patients and do not achieve the target curative effect. In some cases, surgery is not successful in controlling and eliminating all cancer cells in the human body. Moreover, both chemotherapy and radiotherapy may cause harmful effects on normal cells body and poor selection for cancer cells. Recently, with the rise of the nanotechnology star, scientists have improved innovative cancer treatments using nanomaterials. Nanoparticles are particles with dimensions of 1–100 nm. At this size, the physical, chemical, and biological functions of the used material differ highly compared with the material in bulk dimension.

In cancer therapy, the nanomaterials gained the advantage of aggregating in the tumor sites due to the permeability and retention (EPR) effect of tumors larger than normal tissue. Nanosize systems have significant advantages in cancer therapy, starting with their remarkable ability to accumulate at tumor sites, much more than in normal tissues due to the diameter of blood vessels connecting to the tumor is larger than those nourishing the healthy tissue. As a result, the nanosize

* Corresponding author.
** Corresponding author at: Institute of Biological and Chemical Systems – Functional Molecular Systems (IBCS-FMS), Kaiserstrasse 12, Karlsruhe 76131, Germany.
E-mail addresses: aanayel@ju.edu.sa (A.E.A.A. Nayl), stefan.braese@kit.edu (S. Bräse).

https://doi.org/10.1016/j.ijbiomac.2024.138597
Received 19 April 2024; Received in revised form 4 December 2024; Accepted 7 December 2024
Available online 10 December 2024

systems will accumulate in the tumor sites, enhancing the treatment efficiency and minimizing toxicity [1]. Moreover, the nanomaterials' superior optical and electromagnetic properties can be applied as thermal nano-scalpels for killing cancer cells. Through modification of the surface of the nanomaterials, they can be selectively directed to the tumor site, allowing for enhancement of the treatment potential and reducing the side effects [2]. GO nanosheets are 2D materials with only one carbon atom thickness, decorated with different oxygenated function groups (hydroxy, epoxy, ether, diol, and ketone). Allowing multifunctionalities involving biocompatibility, photoluminescence drug loading, and carrier, supposed hopeful medical applications [3]. Polymers were required to graft the GO surface to enhance the biocompatibility of graphene in vivo. Several polymer materials were applied to modify the surface of GO: PEGylated for dual-drug (DOX and platinum) delivery [4], PEI for co-delivery of DOX drug, and p53 tumor suppressor gene for killing HeLa cell [5], PEI grafted GO nanoparticle (PEI-GTC-NP) for carrying of platin and topotecan into mitochondria cancer cells effectively [6]. Owing to their compatibility and degradability, Natural biopolymers are considered appropriate device to develop the biological features of graphene-based materials [7–10].

With anticancer applicability and pH-sensitive, Chitosan has been broadly applied to prepare polymer-graphene composite [11–13]. Chitosan-graphene was prepared for delivery in the Doxorubicin (DOX) drug delivery system. This composite changes its charge in the bloodstream (pH = 7.4) from negative to positive in the tumor tissue (pH 6.5). This behavior leads to separating the chitosan and releasing the DOX. Hyaluronic acid is known as the most polysaccharide that is applied to enhance the biological ability of graphene-based materials [14–16]. Yin's group conjugated hyaluronic acid to GO nanosheet using disulfide bridge to accelerate DOX release in the acidic environment [17].

This paper aims to fabricate a novel (GO-PAA-Cu-LP) nanomaterial as an anticancer agent. The nanomaterial is prepared via a multi-step strategy; first, GO is anchored with PAA via radical polymerization. Subsequently, Na-atom replaced the COOH group's H-atom through interaction with NaOH. After that, Cu-ion was adsorbed to the activated carboxylic groups to serve as a binding site for the purified lactoperoxidase (BLP) from bovine whey. The obtained materials were characterized with several techniques. The activity of prepared materials will be examined against Caco-2 and Huh-7 cell lines of cancer cells.

2. Materials and methods

2.1. Materials

The chemicals required were of analytical grade and utilized without further purification. H2SO4 (95–97 %, Riedelde-Haën), Acrylic acid (98 %, Acros), potassium persulfate (laboratory reagent grade, Fisher Scientific, UK), sodium hydroxide (ACS reagent, ≥97.0 %, pellets, Sigma-Aldrich), Copper(II) sulfate pentahydrate (99.9 %, Sigma-Aldrich), H_2O_2 (36 %, Pharaohs Trading and Import), HCl (30 %, El Salam for Chemical Industries), $KMnO_4$ (99 %, Long live), and graphite (200mesh, 99.99 %, Alpha Aesar).

2.2. Purification of bovine milk lactoperoxidase (LP)

To purify bovine LP, bovine skim milk was defatted by centrifuge (at 5000 r/m) for 30 min and decatenated by decrease the pH value till 4.2 by using 1.0 M HCl [18]. Purification of bovine milk lactoperoxidase (LP) investigated in this work was explained in the Supplementary Material file (Sections 2.2).

2.3. Preparation of GO-PAA-Cu

Firstly, The GO was prepared as reported in our previous work [19]. 150 mg of GO will be dispersed in (10 mL AA/50 mL distilled water) using a hot plate magnetic stirrer to prepare the GO-PAA-Cu. Afterward, 0.4 g potassium persulfate was added to the previous mixture. The temperature of the system was raised to 90 °C for 4 h. The solid phase (GO-PAA) was isolated using a centrifuge and washed with distilled water three times. For activation, the obtained GO-PAA was resuspended in (5 g NaOH/ 500 mL bidistilled water) for another 2 h. The activated composite GO-PAA-Na was separated from the alkali solution by centrifugation at 5000 rpm for 10 min, redispersed in water and centrifuged till neutral pH. Finally, the activated GO-PAA-Na composite was redispersed in ((10 g $CuSO_4$/ 500 mL bidistilled water) for 24 h at 70 °C. The obtained GO-PAA-Cu centrifuge was washed to remove unabsorbed copper ions, lyophilized, and stored for further use.

2.4. Preparation of the modified GO-PAA-Cu-LP composite

The purified lactoperoxidase (LP) was added to GO-PAA-Cu composite for the modification of its surface as follows: resuspended of lyophilized LP (100 mg) in 50 mM phosphate buffer, pH 7.2 was added dropwise to GO-PAA-Cu composite (200 mg) in 50 mL of the same buffer and stirred continuously for 2 h. Then, the modified GO-PAA-Cu-LP were separated by centrifugation at 4000 x*g* (Biofuge primoR, Heraeus, Germany) for 30 min at 4 °C. The obtained pellet was washed three times in 50 mM phosphate buffer, pH 7.2, freeze-dried, and preserved at −4 °C for further use.

2.5. Characterization of the modified GO-PAA-Cu-LP composite

All characterizations of the modified GO-PAA-Cu-LP composite investigated in this study and the measurements of particle size and zeta potential were explained in the Supplementary Material file (Sections 2.5).

2.6. Determination of BLP activity and stability

The activity of the purified LP during purification steps was estimated according to the method of Shindler and Bardsley (1955). The activity of LP was determined based on the ability of LP to oxidize 2,2′-Azino-bis(3-ethylbenzthiazoline-6-sulfonic acid (ABTS) as a chromogenic substrate in the presence of H_2O_2. For enzyme stability estimation, the free or modified form of LP with the prepared GO-PAA-Cu composite was mixed with 1 mM ABTS diluted in 0.1 M phosphate buffer (PH 6.8) in the presence of 3.2 mM H_2O_2 solution. The change in the absorbance was taken at 412 nm as a function of times every 15 s for 3 min. The activity of the free and the modified form of LP was evaluated throughout 9 weeks as described previously [20] to assay the stability of LP during storage conditions at 4 °C. One unit (U) of LP activity was defined as the amount of enzyme catalyzing the oxidation of 1 μmol ABTS per min using a molar absorption coefficient of 32,400 M^{-1} cm^{-1}.

2.7. Dispersibility experiment

In order to improve the biocompatibility of the prepared samples, a concentration of 1 mg/mL of both GO-PAA-Cu and GO-PAA-Cu-LP in water and FBS-containing solution were tested. Thereafter, the powder dispersed in the water and FBS using vortex followed by sonication for 10 min. After that, we evaluated its stability by recording its sedimentation over time up to 6 h.

2.8. In vitro anticancer activity assaying

2.8.1. Cell culture and media

A diploid human normal lung fibroblast (Wi-38), human colorectal adenocarcinoma (Caco-2), and human liver carcinoma (Huh-7) cell lines were obtained from (VACSERA, Cairo, Egypt). DMEM media and fetal bovine serum (FBS) were purchased from (SERANA Co., Germany). Human Wi-38, Caco-2, and Huh-7 cell lines were maintained in a complete DMEM media supplemented with 10 % FBS, 1 % penicillin/

streptomycin, cultured at 37 °C, 88 % humidity, and 5 % CO_2.

2.8.2. Cytotoxicity of the modified composite

The cytotoxic effect of the prepared GO-PAA-Cu and the modified GO-PAA-Cu-LP composite against the tested normal and cancer cell lines was evaluated as discussed in the Supplementary Material file (Section 2.6.2.) [20].

2.8.3. Nuclear staining

The apoptotic effects of the prepared GO-PAA-Cu and the modified GO-PAA-Cu-LP against Caco-2 cells were evaluated using double fluorescent stain method by acridine orange and ethidium bromide (AO/EB) dyes for staining nuclei of the treated cells in comparison with untreated reference cells. In Brief, the treated-Caco-2 cells were washed 3 times with DMEM fresh media and fixed with 4 % paraformaldehyde for 10 min. The cells were permeabilized by adding 3 % paraformaldehyde containing 0.5 % Triton X-100 for 1 min. Then, 10 μg/mL of each AO/EB dye solution was added for staining the tested cells for 20 min in the dark condition. The cells were visualized and photographed using a fluorescence phase contrast microscope (Olympus, Japan) at an excitation filter of 480/30 nm.

2.8.4. Cell cycle analysis

The flow cytometry, FACS (Partec, Germany), was used to evaluate the effect of the prepared GO-PAA-Cu-LP in the distribution of the cancer cell cycle phases. Caco-2 cells were treated with the prepared samples at optimum conditions as discussed in the Supplementary Material file (Section 2.6.4.). The cells were detached and fixed as explained in the Supplementary Material file (Section 2.6.4.).

2.9. Effect of the modified GO-PAA-Cu and GO-PAA-Cu-LP NPs on gene expression

The effect of the prepared GO-PAA-Cu and the modified GO-PAA-Cu-LP on the expression level of some tumor genes, including tumor suppressor gene (p53), Caspase-9, interleukin-6 (IL-6) and oncogene (Bcl-2) was investigated in this work as explained in the Supplementary Material file (Sections 2.7.).

2.10. Statistical analysis

Data were expressed as mean ± standard deviation (SD). The multiple comparisons determined statistical significance, and the obtained data were estimated using the multiple comparisons Tukey post-hoc analysis of variance (ANOVA) using the SPSS16 program. The differences were considered statistically significant at $p < 0.05$.

3. Results and discussions

3.1. Characterization of the prepared GO-PAA-Cu-LP composite

Bovine milk possesses many proteins that are recognized as potent anticancer agents. Therefore, there is a vital demand for improving their stability and protecting them from body barriers. It is essential to deliver these proteins to target cancer sites using many technologies, such as nanomedicine, besides boosting their bioactive purposes via nanoformulations with nanometals [21]. Bovine LP is a monomeric heme-containing protein that can chelate calcium and iron [22,23]. Bovine LP is a positively charged enzyme with isoelectric point (pI) estimated to be 9.6, and this significant positivity is a property of the main essential properties of its structural; it has important biological functions, including immunomodulatory roles and antimicrobial efficiency [24]. Bovine LP is translated as a preproprotein consisting of 612 residues which included the N-terminal peptide of about 20 amino acids, a propeptide of about 100 to 300 amino acids, and a catalytic domain. The mature BLP contains 15 cysteines (Cys) inside its amino acids sequence that form 7 disulfide bonds; Cys6-Cys167, Cys15-Cys28, Cys129-Cys139, Cys133-Cys157, Cys237-Cys248, Cys456-Cys513, and Cys554-Cys579, whereas the Cys441 remains as a free cysteine residue [25]. The adsorption of the protein on the surface of the NP's created a novel combination called NP-protein complexes, which explains NPs bioreactivity. This is due to, the variation of the protein structure after adsorption on the NPs surface which may leading to change the main property of the protein [26].

After defatting and decasination of bovine milk to obtain skimmed milk, BLP was purified from skimmed milk through two simple purification steps using cation and size exclusion column chromatography. Bovine skimmed milk was applied into a pre-equilibrated cation exchange Mono S 5/50 GL column with phosphate buffer (50 mM, pH 7.0), and BLP was eluted from the column using a 0.0–1.0 M NaCl gradient. All fractions positive for BLP activity were pooled and dialyzed against phosphate buffer (50 mM, pH 7.0). Mono S column was used to purify BLP using a 0.0–0.6 M NaCl gradient. All BLP fractions were pooled, concentrated, and desalted using ultrafiltration centric on with cut-off 30 kDa. The dialyzed LP-containing fractions were uploaded to size exclusion Sephacryl S100 column chromatography, and BLP was eluted using 0.05 M phosphate buffer, pH 7.0 containing 0.15 M NaCl. Homogeneity and purity of the purified BLP were visualized by 12 % SDS-PAGE [18]. The nanocomposites GO-PAA-Cu were prepared by grafting PAA on the surface of GO through radical polymerization, followed by activation by treating them with NaOH aqueous solution. The activated composite was suspended in Cu^{+} ion solution to adsorb the Cu^{+}-ions on the active sites to yield GO-PAA-Cu nanocomposite. Finally, the obtained composite reacts with BLP in phosphate buffer to produce the target GO-PAA-Cu-LP (Fig. 1). The GO-PAA-Cu-LP nanocomposite connected with water due to LP is hydrophilic materials which will make the surface of GO-PAA-Cu-LP nanocomposite hydrophilic. This will cause the nanocomposite connected to the water molecules in the aqueous solution. Additionally, the modified GO-PAA-Cu-LP composite possessed high sedimentation rate due to the agglomeration of the GO layers because of its modification process.

The SEM and TEM were applied to detect the morphological structure of the prepared composites. The SEM of GO-PAA-Cu showed an agglomerated layered structure, possibly due to the action of Cu^{2+} ion that crosslinked the polymer chains that decorated the GO layer, leading to agglomeration (Fig. 2a-c). By treating the GO-PAA-Cu with BLP, the Cu^{2+} ions will act as a bridge to link the BLP molecule to the GO-PAA-Cu surface and compose GO-PAA-Cu-LP. This will break down the agglomeration, and the GO-PAA-Cu-LP will appear in an ideal layered structure (Fig. 2 d-f). The TEM images of GO-PAA-Cu appear as multilayered GO with aggregates spread on its surface, which may be referred to as PAA-Cu (Fig. 3 a-c). The TEM images of GO-PAA-Cu-LP, in which a bulky dark particle (may be BLP molecules) were observed associated with the GO-PAA-Cu nanocomposite surface (Fig. 3 d-f). In the current study, we approved that the interaction of the BLP and GO-PAA-Cu to prepare GO-PAA-Cu-LP complex, which improves the activity of BLP, hinting at its application as an antitumor candidate for fighting different types of cancer and usage in the medical field.

In contrast, SEM and TEM results improved that there are small PAA-Cu and PAA-Cu-LP nanoparticles on the surface of GO (Figs. 2 and 3), that might be for interaction of the PAA polymer species and Cu-ion. After that the interaction among the LP and the adsorbed Cu-ion on the GO-surface. In the same agreement, Li et al., [27] demonstrated that the modified NGO-PEG-NH-1 act as a carrier for doxorubicin, which leading to formation small NPs on the surface of GO that related HN-1 peptide.

The TEM-EDX was considered an efficient tool to estimate the elements that composed the target materials. The TEM-EDX of GO-PAA-Cu nanocomposite showed that it is composed of C, O, Na, and Cu, which confirms the preparation process (Fig. 4a). After loading LP, several elements such as N, O, P, S, Cl, etc., were noted in the EDX sheet of GO-PAA-Cu-LP which affirmed the successful loading of BLP molecule over

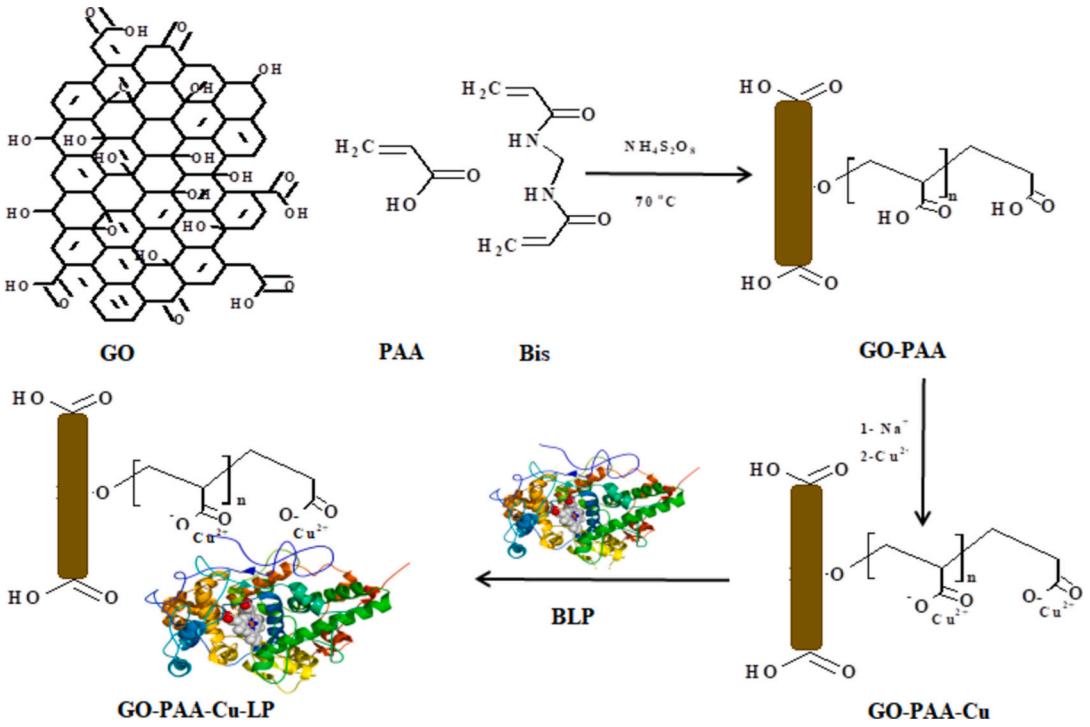

Fig. 1. Illustration diagram show the interacting of BLP enzyme with the prepared GO-PAA-Cu composite forming the modified GO-PAA-Cu-LP composite.

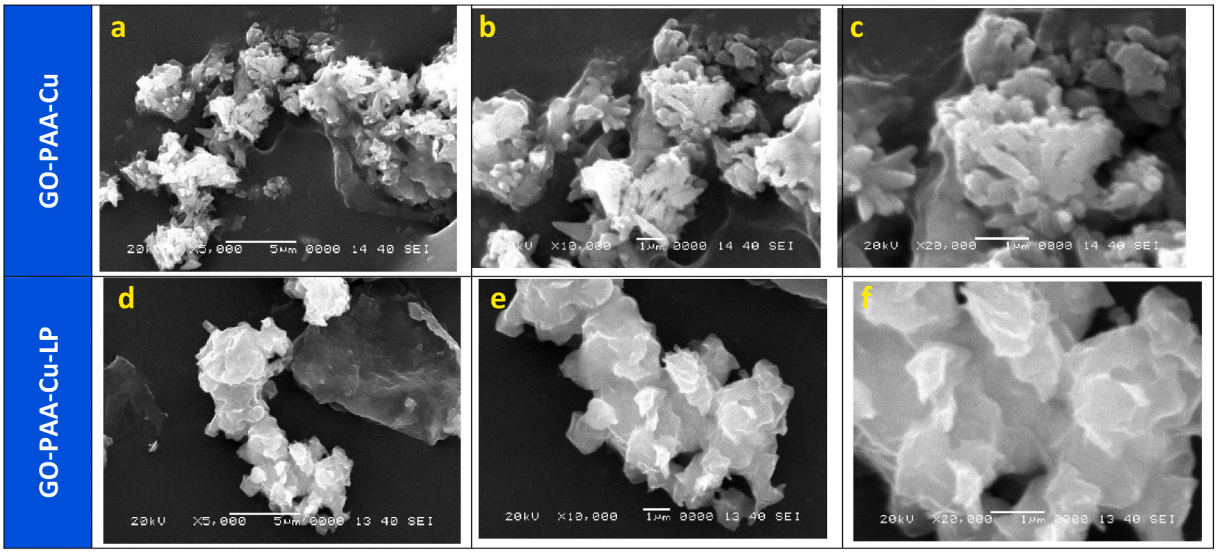

Fig. 2. SEM images of the synthesized GO-PAA-Cu (a-e) and the modified GO-PAA-Cu-LP (f-k) at different magnifications.

the GO-PAA-Cu (Fig. 4b).

Fig. 5a pointed to the FTIR of GO, GO-PAA-Cu and GO-PAA-Cu-LP. The GO shows its characteristics peaks at 3428 cm^{-1} (O—H stretching), 1642 cm^{-1} (water bending), 1403 cm^{-1} (C═O deformation) and 1074 cm^{-1} (C—O stretching). By modification of the GO with PAA—Cu, the peak due to absorbing water highly shit to 3221 cm^{-1}, new peak due to C—H stretching was obtained at 2920 cm^{-1}, the band at 1642 cm^{-1} disappeared, a new band at 1541 cm^{-1} attributed to asymmetric stretching of COO^{-} was obtained, the band at 1403 cm^{-1} was shifted to 1373 cm^{-1}, finally, new peak due to Cu—O stretching appeared at 517 cm^{-1}. After loading LP, the GO-PAA-Cu-LP shows the same peaks related to GO-PAA-Cu but with low intensities.

TGA was utilized for determining the thermal stabilities of the assessed materials. The thermal stabilities of GO, GO-PAA-Cu and GO-PAA-Cu-LP was studied as in (Fig. 5b). As observed, the GO decomposed over four steps due to evaporation of surface water, interlayer water, pyrolysis of oxygenated function groups like as OH and COOH as shown in (Fig. 5b). After modification the GO with PAA and followed by loading Cu ions, the thermal of GO-PAA-Cu will be delayed from 152 °C in case of pure GO to 313 °C for GO-PAA-Cu nanocomposite due to covering the GO surface with the PAA polymer chains which provide high stability for the prepared composite (Fig. 5b). Moreover, the main decomposition step for the pure GO (22 %, 152–215 °C) will be highly enhanced in case of GO-PAA-Cu (36 %, 314–422 °C). This may be referred to as the presence of Cu ion, which will catalyze GO-PAA-Cu decomposition at elevated temperatures. The LP will cover the composite and isolate it from the temperature effect by treating the GO-PAA-Cu-Cu with LP to form GO-PAA-Cu-LP. Thus, the GO-PAA-Cu-LP will

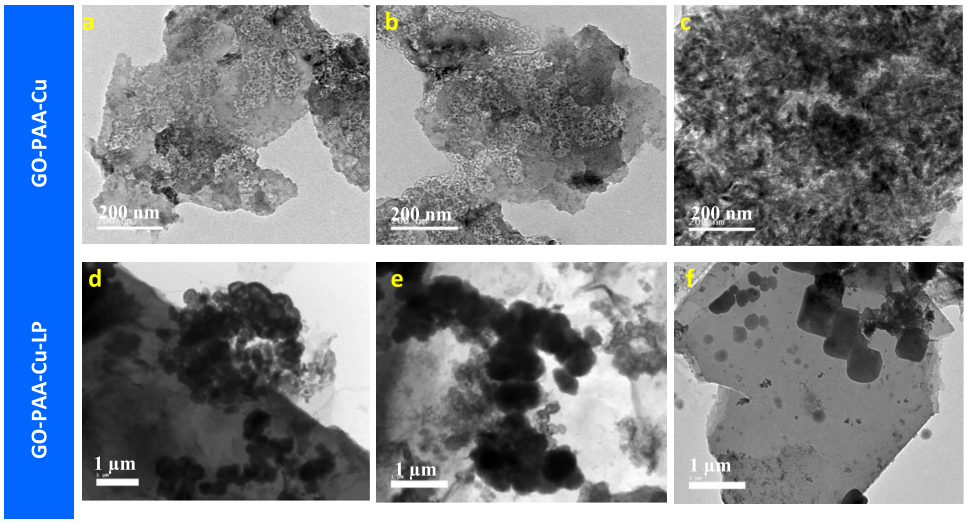

Fig. 3. TEM images of the synthesized GO-PAA-Cu (a-c) and the modified GO-PAA-Cu-LP (d-f).

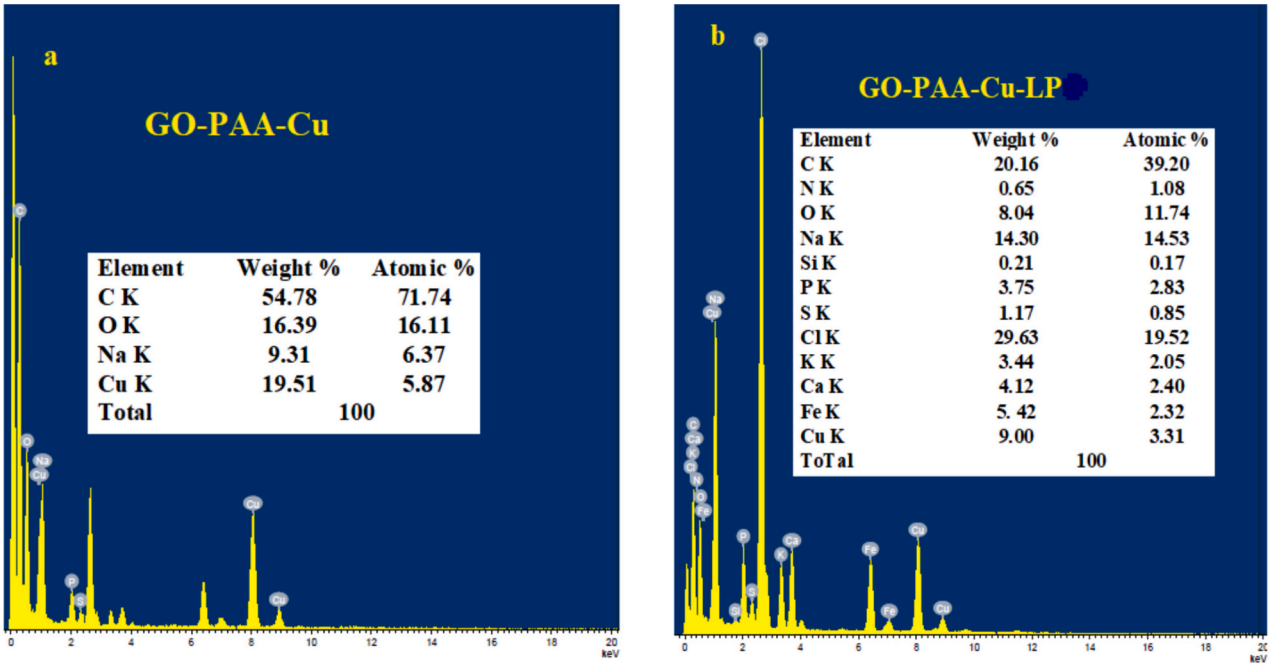

Fig. 4. TEM-EDS of a) GO-PAA-Cu and b) GO-PAA-Cu-LP.

present a gradual degradation regime over the applied temperature range, see Fig. 5b.

XRD was used to detect the crystal structure of fabricated materials. The XRD patterns of GO, GO-PAA-Cu, and GO-PAA-Cu-LP are noted in Fig. 5C. The GO shows its characteristic sharp, intense peak at $2\theta = 10^{o}$. After modification of the GO with PAA—Cu, the sharp, intense peak of the GO disappears, and a broad, weak peak appears at $2\theta = 22^{o}$. Moreover, the loading of LP over GO-PAA-Cu will not highly alter the XRD pattern from GO-PAA-Cu. As obtained findings, BLP interacted with GO-PAA-Cu composite and formed a hard corona owing to many reasons, involving the structure of LP contains many basic amino acids with high positive charges such as Lys and Arg residues, besides the high cationic of LP, which enhances its binding to GO-PAA-Cu composite. Also, cysteine residues found in the LP structure have an S—H group, increasing the LP linkage on the GO-PAA-Cu surface.

3.2. Zeta potential and particle size

The particle size and zeta potential of GO-PAA-Cu and GO-PAA-Cu-LP were investigated, as shown in Fig. 6 (A and B). The GO-PAA-Cu possessed a particle size of 2016 nm and Zeta Potential (−13.4 mV), see Fig. 6A(I, II). Upon loading the positively charged LP molecules, the Cu will be utilized as a satellite to attach the LP by the composite surface. This will generate a small particle on the surface of the GO of size 185 nm with percent (9.7 %), as illustrated in Fig. 6(BI), refer the TEM images (Fig. 3d-f). Moreover, we could be observed that, the allover particle size and the zeta potential of the GO-PAA-Cu-LP will be reduced to 1114 nm and − 10.4 mV, respectively, as illustrated in Fig. 6A(II) and 6B (II), respectively.

3.3. Stability of the purified bovine lactoperoxidase

The LP activity and stability in the free and modified forms were

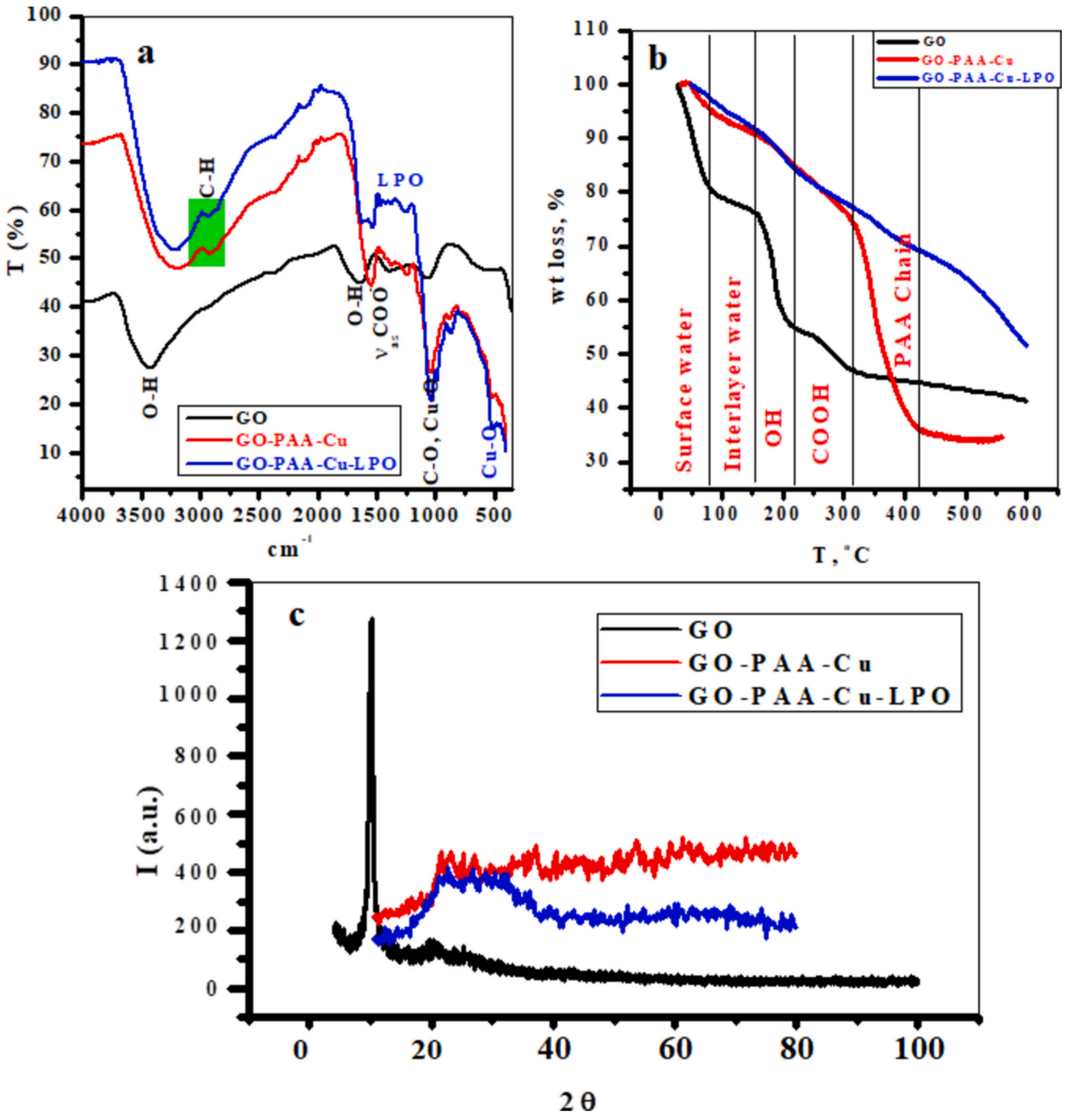

Fig. 5. a) FTIR spectra, b) TGA, and c) XRD pattern of GO, GO-PAA-Cu, and GO-PAA-Cu-LP.

determined by assaying the activity of LP during cold storage in a refrigerator for 9 weeks at 4 °C. The activity of the purified LP in free form decreased steadily by increasing the storage time until it became 0 after 6 weeks of storage at 4 °C (Table 1). While, the reactivity of LP in the modified form (GO-PAA-Cu-LP composite) maintained at 73 % of its initial activity after 9 weeks of storage at 4 °C (Table 1). Therefore, the modified form of LP retained its activity more than the free form after storage for 9 weeks at 4 °C. Any enzyme's activity and stability are usually affected through the immobilization process based on the methods used, such as entrapment and adsorption approaches. Depending on this observation, here, unlike LP entrapment, the adsorption of BLP on the surface of GO-PAA-Cu-LP composite did not increase its activity but improved its stability rather than free enzyme, which may be owing to alter of its chemical and physical structure as well as change of whole surface microenvironment. All these reasons may affect the kinetic parameters of the adsorbed enzyme without changing the tertiary structure of substrate binding sites and maintaining its activity.

Meanwhile, the adsorption of BLP on the surface of nanocomposite may occur by the combination of enzymatic residues and functional groups of GO-PAA-Cu composite that are away from the active and substrate binding sites without affecting its proper surface microenvironment [28]. Therefore, the modified GO-PAA-Cu-LP composite could maintain LP activity longer than free BLP form. This observation was in touch with the data obtained by Nayeri et al. [29], who noted that LP-encapsulated tragacanth-chitosan NPs will enhance the stability of LP

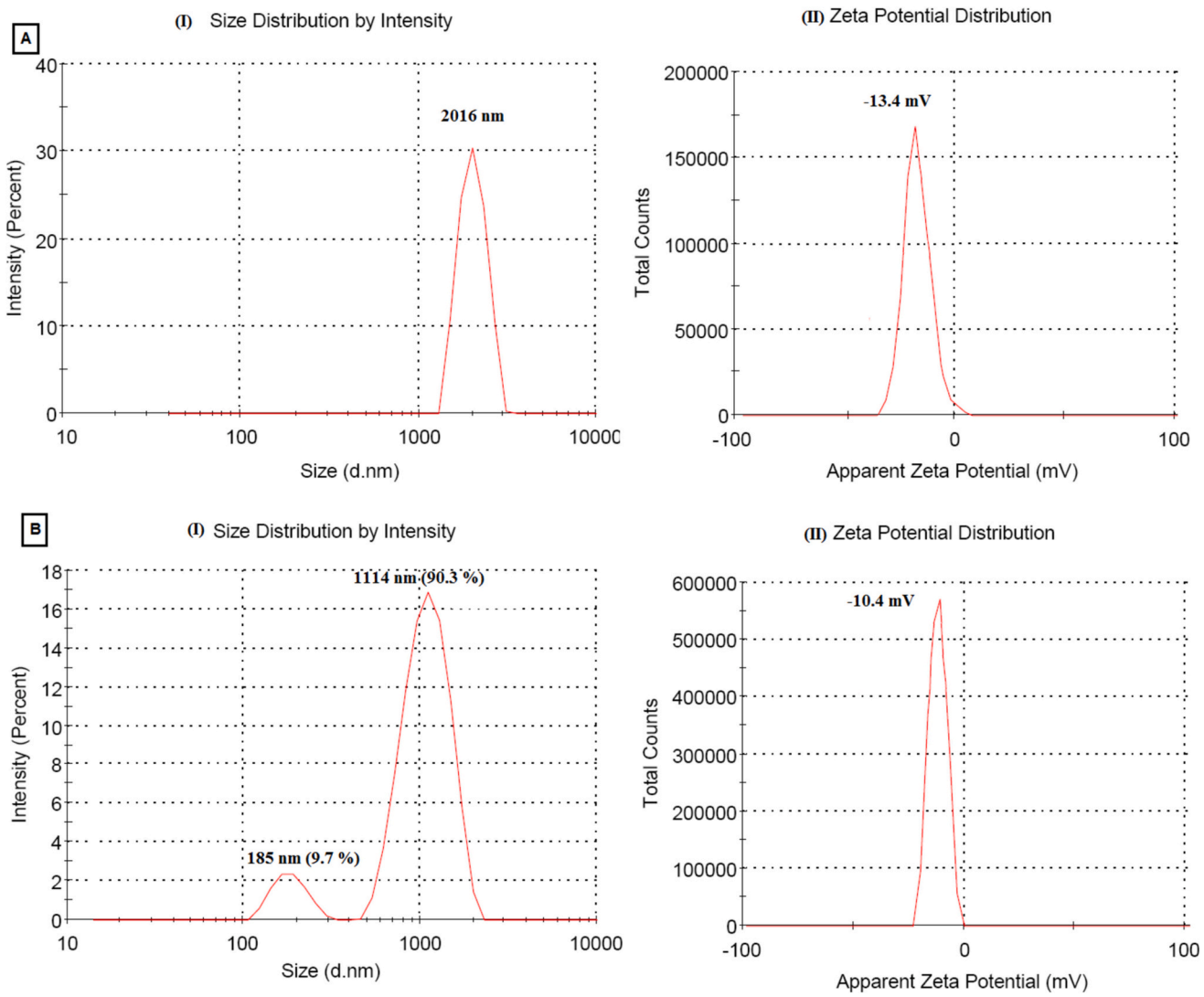

Fig. 6. Average particle size (AI, BI) and Zeta potential (AII, BII) of GO-PAA-Cu and GO-PAA-Cu-LP nanocomposites, respectively.

Table 1
Stability of the purified bovine LP activity (IU) as free and modified (GO-PAA-Cu-LP composite) forms during 9 weeks of storage at 4 °C.

Week	1	2	3	4	5	6	7	8	9
BLP	65.87 ± 4.09a	50.22 ± 3.81ab	31.45 ± 2.76ab	8.59 ± 0.65b	3.86 ± 0.32b	0.0	0.0	0.0	0.0
GO-PAA-Cu-LP	67.23 ± 5.47a	61.19 ± 4.92a	55.17 ± 4.16a	49.14 ± 4.28a	46.56 ± 3.94a	42.39 ± 3.65a	40.09 ± 3.14b	36.62 ± 2.85b	34.59 ± 3.41c

All results are represented as mean ± SD, and letters differ significantly within the same raw at $p < 0.05$.

than the free LP at +4 °C and 25 °C for 14 days and when heating to about 80 °C.

3.4. The results of the stability experiment

To mimic the blood environment in-vivo, we follow the dispersibility of the prepared GO-PAA-Cu and GO-PAA-Cu-LP nanocomposites in both water and FBS-containing solution. Referring to the Fig. 7, the both nanocomposites (GO-PAA-Cu and GO-PAA-Cu-LP) showed excellent suspension ability in FBS over 6 h. Further, the sedimentation behavior of both composites is neglected after standing for 3 h (Fig. 7). Thereafter, the both composites (GO-PAA-Cu and GO-PAA-Cu-LP) slowly precipitate till 6 h. Similarly, by using distilled water as dispersion medium, the both nanocomposites (GO-PAA-Cu and GO-PAA-Cu-LP) possessed enhanced suspension ability in water over 3 h (Fig. 7). This is attributed to in case of GO-PAA-Cu; an ionic bond may be formed among the Cu-ion and the O-atom of the water ($Cu^{+\delta}....^{-\delta}OH_2$). After loading of LP, the LP involved on high dense of the function groups (NH_2, COOH) which may be interact with the water molecules with (H-bond) (LP….H-O-H). This can be observed from the FTIR graph (Fig. 5a) which present high intensity of the O—H stretching band at 3428 cm^{-1}. Then the both nanocomposites starts to sediment and a precipitation starts to appear at the bottom of the tubes, see Fig. 7.

3.5. Anticancer activity of the modified GO-PAA-Cu-LP

In the present in vitro study, the modified form of LP on the surface of GO-PAA-Cu composite was tested for its anticancer effect against different types of cancer cells compared to free for LP and the free form of the prepared GO-PAA-Cu composite. The safe doses (EC_{100}) of GO-

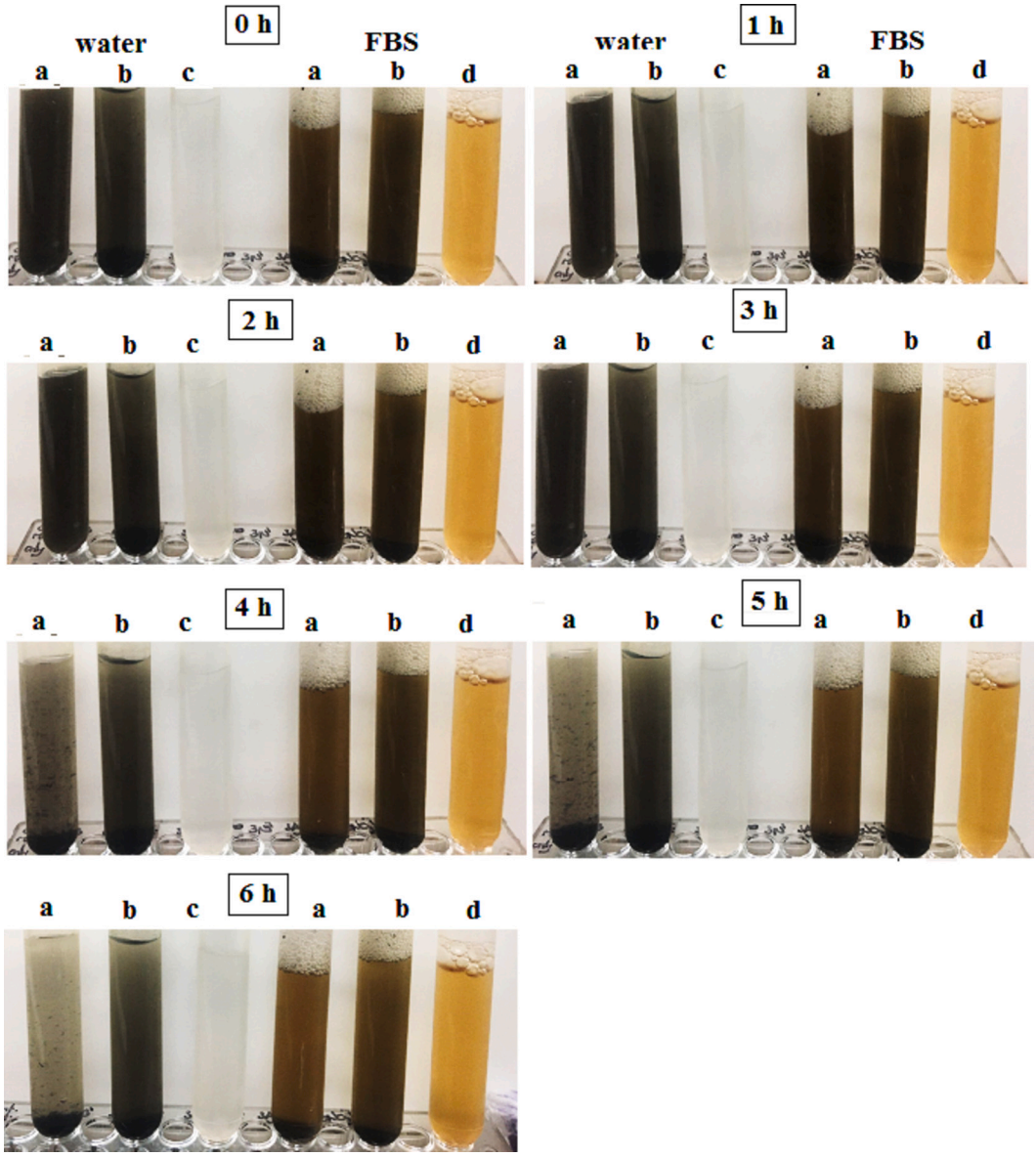

Fig. 7. The results of the dispersibility experiment of GO-PAA-Cu-LP (a) and GO-PAA-Cu (b) nanocomposites in water (c) and FBS (d) at concentration of 1 mg/mL.

PAA-Cu composite, the modified GO-PAA-Cu-LP composite, and free LP that retained 100 % viability of the tested normal Wi-38 cell line were 10.74, 68.99, and 79.77 μg/mL, respectively. While their EC_{100} values against the cancer Caco-2 cell line were 65.67, 6.14, and 34.98 μg/mL, and against the cancer Huh-7 cell line, were 56.24, 5.39 and 31.35 μg/mL, respectively (Table 2). The IC_{50} values against Caco-2 cells were 194.2, 349.7, and 1323 μg/mL, and against Huh-7 cells, were 170.5, 313.4, and 1133 μg/mL for the free GO-PAA-Cu composite, the modified GO-PAA-Cu-LP composite and free LP, respectively (Table 2). It has been revealed that the selectivity against both treated Caco-2 and Huh-7 cell lines of the modified GO-PAA-Cu-LP composite is greater than the prepared free GO-PAA-Cu composite and free LP. Thus, the selectivity index for the modified GO-PAA-Cu-LP composite was determined to be 3.13 and 3.49 against Caco-2 and Huh-7 cell lines, respectively. Therefore,

Table 2
EC_{100}, IC_{50} (μg/mL), and SI values of the purified BLP, GO-PAA-Cu composite, and the modified GO-PAA-Cu-LP composite against Wi-38, Caco-2, and Huh-7 cell lines after treatment for 48 h.

Cell lines		The purified LP	GO-PAA-Cu composite	The modified GO-PAA-Cu-LP composite
Wi-38	EC_{100}	79.77 ± 6.63	10.74 ± 0.38	68.99 ± 2.84
	IC_{50}	1607 ± 133.6	339.5 ± 12.06	1093 ± 28.39
Caco-2	EC_{100}	65.67 ± 3.56	6.14 ± 0.56	34.98 ± 2.29
	IC_{50}	1323 ± 35.68	194.2 ± 17.59	349.7 ± 22.97
	SI	1.21 ± 0.10	1.75 ± 0.06	3.13 ± 0.08
Huh-7	EC_{100}	56.24 ± 3.45	5.39 ± 0.49	31.35 ± 2.42
	IC_{50}	1133 ± 34.53	170.5 ± 15.74	313.4 ± 24.26
	SI	1.42 ± 0.12	1.99 ± 0.07	3.49 ± 0.09

All data were expressed as mean ± SD.

the strongest potential selectivity against all tested cancer cells was demonstrated by the modified GO-PAA-Cu-LP composite. Fig. 8A represents a high safety of the modified GO-PAA-Cu-LP composite against the tested normal human lung fibroblast (Wi-38) cells as compared to the free GO-PAA-Cu composite, which showed great cytotoxicity on the treated cancer cells. However, both the modified GO-PAA-Cu-LP composite and GO-PAA-Cu composite showed a great anticancer effect on both treated Caco-2 and Huh-7 cells as compared to the free LP, which showed the lowest anticancer activity (Fig. 8B and C).

Therefore, these results indicate that the coating of LP on the surface of GO-PAA-Cu composite increased its selectivity against all treated cancer cell lines.

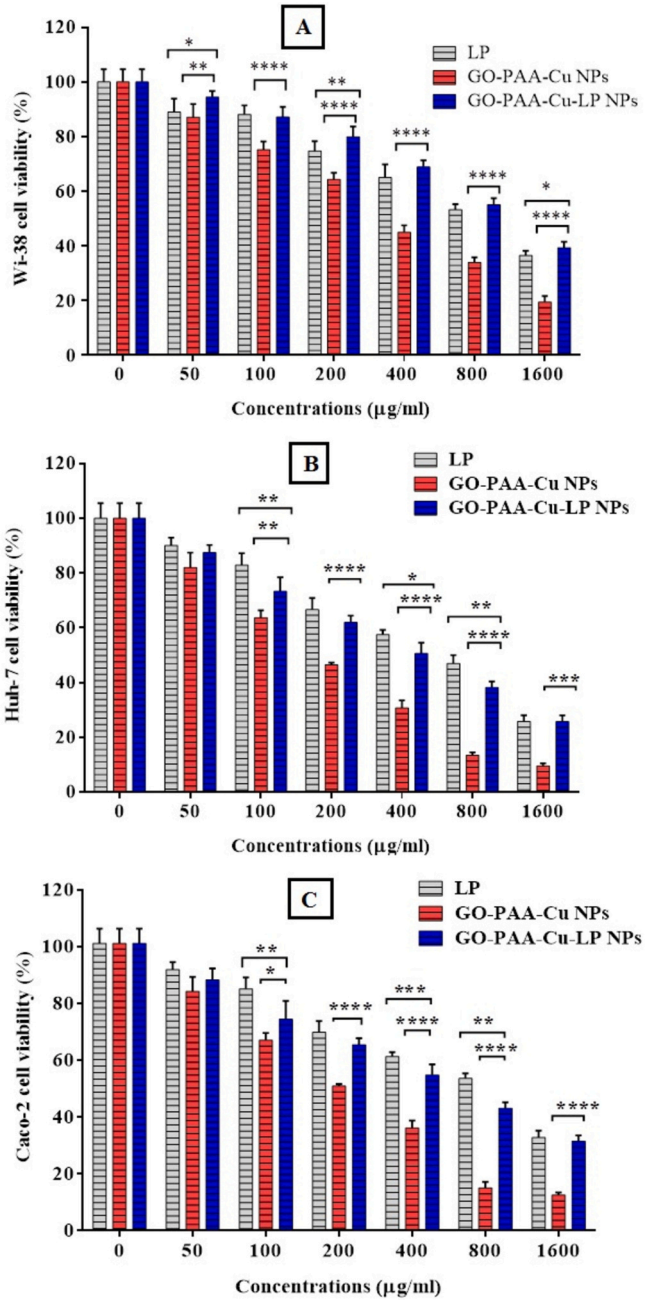

Fig. 8. The cytotoxicity profile of the prepared GO-PAA-Cu NPs and the modified GO-PAA-Cu-LP NPs against the normal Wi-38 cells (A), colon cancer Caco-2 cells (B), and liver cancer Huh-7 cells (C). All treated cells were incubated with the prepared and modified NPs at different concentrations (0–1600 µg/mL) for 48 h. All data are represented as mean ± SD and represent the average values from three experiments ($n = 3$), and data were considered significantly different at $p < 0.05$ *, $p < 0.005$ **, $p < 0.0005$ ***, $p < 0.0001$ ****.

Interestingly, numerous studies have been performed to investigate the safety of LP in many mammalian cells. Hänström et al. [30] demonstrated that several mixtures of LP-SCN-H_2O_2 did not show any cytotoxicity against many tested cell lines, including human epidermoid carcinoma of the cervix cell line (HeLa), human gingival fibroblasts and a Chinese hamster ovary cell line (CHO). Kim et al. [31] demonstrated that the toxicity of the mode of silica NPs was dependent on their dose, size, and cell kind.

The previous study conducted by El-Fakharany et al. [18] indicated that the modified BLP on the surface of silica NPs showed slight cytotoxicity against mammalian fibroblast cells at high concentrations with an IC_{50} value of 2.8 mg/mL. Furthermore, Abu-Serie and El-Fakharany [20] revealed that both coated and loaded LP to chitosan NPs demonstrated a safe manner on the tested normal cells.

In addition, this prepared complex (GO-PAA-Cu-LP) showed a potent anticancer against the Huh-7 cell line more than the Caco-2 cell line. Copper ion is one of the heavy metals that, at low concentrations, is well-identified to be shared in many metabolic processes and cellular functions; however, at high levels, it can deserve undesirable effects [32]. Furthermore, nanometals show high stability in harsh environments such as temperature; pH intensifies, increasing their use in many medical fields. In this study, the synergistic efficacy of the grafted BLP with GO-PAA-Cu composite might contribute to the absorbed enzyme's stability after conjugation with GO-PAA-Cu on its surface. Also, this strong cytotoxicity may result from the variation to the whole bio-reactivity of the modified composite.

Additionally, the high positivity of the BLP-coated GO-PAA-Cu composite assist in cancer cell membrane disruption in a high selectivity manner with great safety toward normal surrounding cells. This high selectivity toward tumor cells owing to the negative charge of the tumor cell membrane compared with normal cells, which enhances their linking to the cationic proteins and components, causing the rupture of the target tumor cells sparing normal cells and tissues [33]. To the best of our knowledge, the present investigation is the first to study the enhancement of the antitumor efficacy of the modified BLP by absorbing or coating GO-PAA-Cu composite against both hepatoma and colon carcinoma cells. We can deduce that modifying GO-PAA-Cu composite with BLP enhanced their synergetic effect against the tested tumor cell lines and improved their safety against surrounded normal cells. Hence, absorbing or coating BLP on the prepared composite's surface strongly boosted their selectivity against cancer cells more than free single BLP and GO-PAA-Cu composite. This agrees with [20], who demonstrated that LP and/or LF absorption onto chitosan NPs maintained LP stability and activity more than the free form of protein with enhanced anticancer activity against numerous treated cells. On the other hand, the combination of LP with NPs, by coating or loading, boosts additional stability to LP.

3.6. Apoptotic activity of the modified GO-PAA-Cu-LP composite

More interestingly, Fig. 9A exhibits the observations of the morphological structure of the treated Caco-2 cells with the modified GO-PAA-Cu-LP composite and free GO-PAA-Cu composite at various concentrations of (100, 200, and 400 µg/mL) for 48 h as compared to untreated cells and treatment with free LP. The morphological changes of the treated Caco-2 cells included the induction of cell destruction with complete collapse of their spindle morphology, cell shrinkage, and nuclear condensation, which is proportionally enhanced with the dose of the treatment (Fig. 9A). The obtained results proved the strongest apoptotic effect of the modified GO-PAA-Cu-LP composite among all examined compounds. On the other hand, the apoptotic effect of the prepared compounds was cleared with double acridine orange/ethidium bromide (AO/EB) nuclear staining and visualized under a fluorescence phase contrast microscope (Fig. 9B). The treated Caco-2 cells

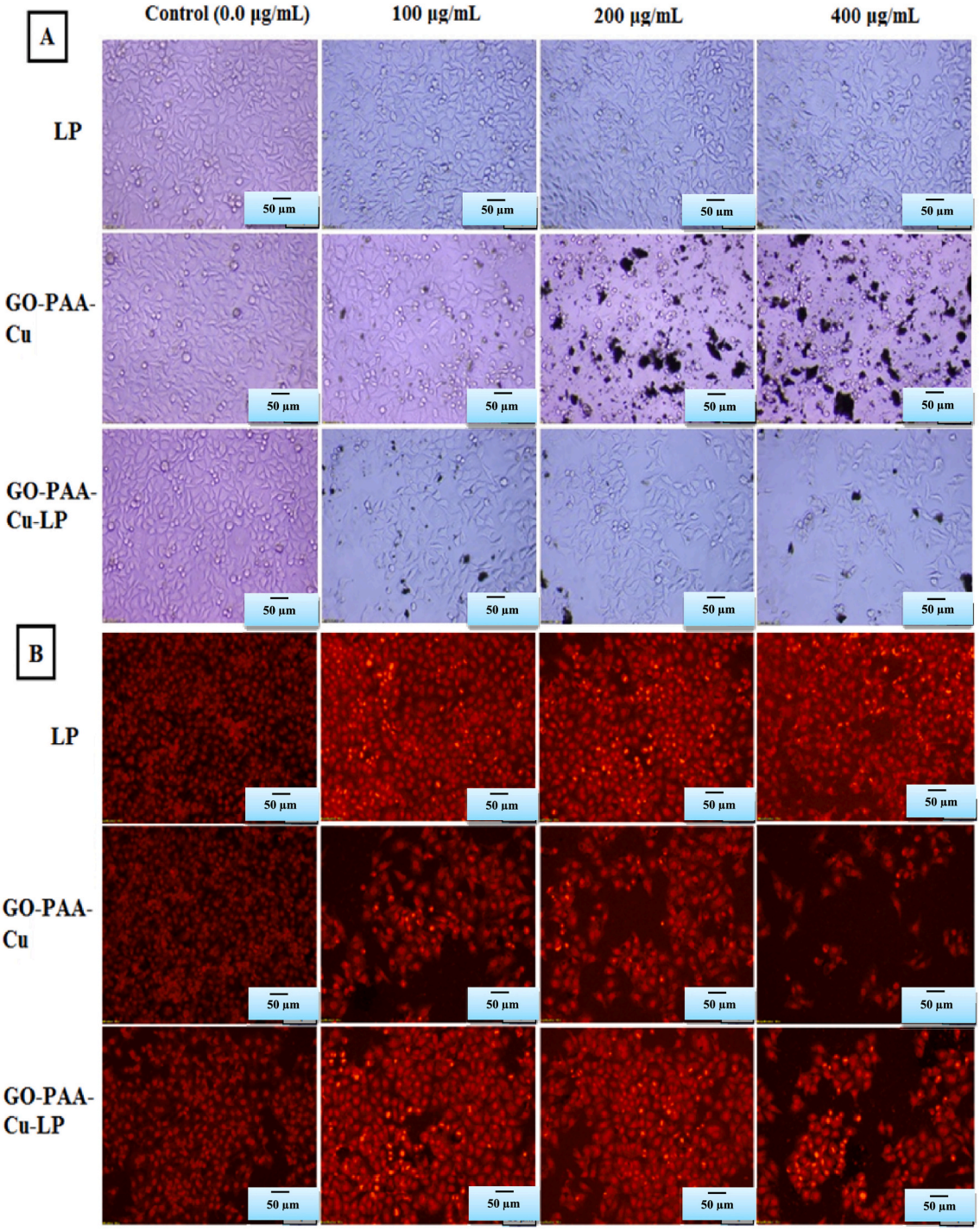

Fig. 9. Effect of the prepared GO-PAA-Cu composite and the modified GO-PAA-Cu-LP composite on the morphological and nuclear changes of cancer Caco-2 cell line compared to the purified LP. (A) Micrographs of the treated Caco-2 cells were captured by an inverted phase contrast microscope. (B) Investigation of the apoptotic effect of treated Caco-2 cells with free LP, GO-PAA-Cu composite, and the modified GO-PAA-Cu-LP composite using double fluorescence staining (AO-EB) compared to control (untreated) Caco-2 cells. Caco-2 cells were exposed to 100, 200, and 400 µg/mL of each sample for 48 h, and untreated (control) cells were included as negative references. All experiments were performed three times, Magnification 100 X and scale bar 50 µm.

ascertained fluorescence ranging from yellow to red when comparison with the untreated viable (control) cells that ascertained green.

fluorescence. The low apoptotic effect of the free LP was confirmed by ascertaining the yellow fluorescence of the treated cancer cells, which proved the incidence of apoptotic effect was exerted at an early stage. However, the nuclei of the treated Caco-2 cells with the modified GO-PAA-Cu-LP composite and free GO-PAA-Cu composite showed the incidence of yellow and orange fluorescence, which proved a high apoptotic effect. Notably, some treated cells with the modified GO-PAA-Cu-LP composite and free GO-PAA-Cu composite lost their cellular integrity by emitting red fluorescence, indicating the incidence of apoptotic effect at a late stage (Fig. 9B). Moreover, the effect of the modified GO-PAA-Cu-LP composite and free GO-PAA-Cu composite on cell cycle arrest in Caco-2 cells was investigated to advance insight into the potential mechanisms of these compounds that provoke the apoptotic effect on the cancer cells. Caco-2 cells were treated with the

modified and free composites at IC_{50} doses for 48 h and stained with PI to determine the cell cycle phases using flow cytometer analysis. Fig. 10A shows the capability of the modified GO-PAA-Cu-LP composite to induce the arrest of cell cycle profile in both G0/G1 and G2/M (two main checkpoint phases) of cell population growth more than both free GO-PAA-Cu composite and LP. The obtained results demonstrated that the treatment increased the percentage of the apoptotic phase (sub-G1) population, while the S phase (synthesis checkpoint) was decreased as compared to untreated viable cells (Fig. 10A1 and 10A2). These results indicate that the modified GO-PAA-Cu-LP composite enhanced cell cycle arrest of treated cancer cells in both the sub-G1 phase (apoptotic phase) and the S phase compared with untreated (control) cells, stimulating apoptotic mechanism.

In addition, Fig. 10B indicates that the modified GO-PAA-Cu-LP composite can up-regulate the apoptotic p53 and Caspase-9 genes in the treated Caco-2 (Fig. 10B1), Huh-7 (Fig. 10B2), down-regulate anti-apoptotic gene (BCl-2) and suppress the expression of pro-inflammatory gene (IL-6) in both treated cell lines also. It was observed that the modified GO-PAA-Cu-LP composite at IC_{50} dose present the largest effect on up-regulation of both p53 and Caspase-9 genes in both Caco-2- and Huh-7-treated cells more than the treated cells with the free GO-PAA-Cu composite and LP. Also, the modified GO-PAA-Cu-LP composite showed the highest suppression effect of the expression level of both BCl-2 and IL-6 genes. The expression level of p53 in the GO-PAA-Cu-LP treated cells was found to be >5–6 times larger than control cells and 2–2.5 times compared to the GO-PAA-Cu treated cells. At the same time, the expression level of Caspase-9 was activated by treatment with the modified form to be about 4 folds more than the untreated control cells and about 2 folds as compared to the GO-PAA-Cu treated cells. The expression levels of Bcl-2 and IL-6 genes in both treated cancer cells with

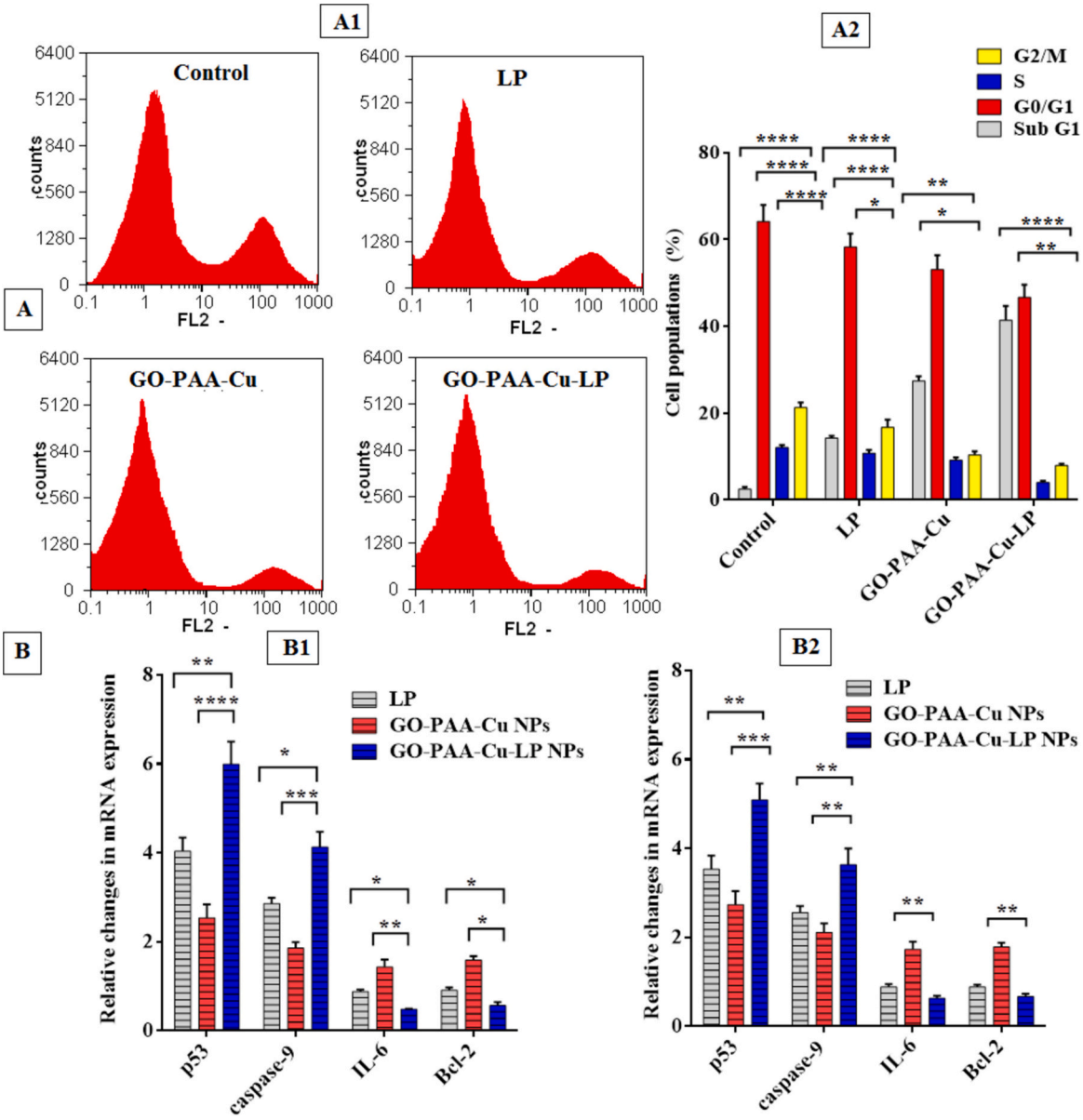

Fig. 10. Apoptotic effect of GO-PAA-Cu composite and the modified GO-PAA-Cu-LP composite against cancer cells. (A) Cell cycle profile of the treated Caco-2 cells with LP, GO-PAA-Cu composite, and the modified GO-PAA-Cu-LP composite, (I) cell cycle distribution diagrams (original flow charts), and (II) quantitative distribution of the treated Caco-2 cells in different phases of the cell cycle compared with untreated (control) cells. (B) Relative fold change of gene expression levels of p53, Caspase-9, IL-6, and Bcl-2 in the treated Huh-7 cells (B1) and Caco-2 cells (B2) after treatment for 48 h with GO-PAA-Cu composite and the modified GO-PAA-Cu-LP composite in comparison with LP. All values are demonstrated as mean ± SD. represent the average values from three experiments ($n = 3$) and data were considered significantly different at $p < 0.05$ *, $p < 0.005$ **, $p < 0.0005$ ***.

the modified GO-PAA-Cu-LP composite were found to be suppressed with more 1.5 folds than the untreated cells. However, more than in untreated cells, Bcl-2 and IL-6 genes were overexpressed in GO-PAA-Cu composite-treated Caco-2 and Huh-7 cells.

Herein, the modified GO-PAA-Cu-LP composite has a potent apoptotic effect that may be exerted through its high oxidation activity as a result of the generation of the activated O-species such as $HOO^{\bullet}$, $O^{2\bullet}$, $HO^{\bullet}$, and HOO^{-} in the surrounded media. These activated O-species are considered extremely non-selective and strong oxidants [34]. This hypothesis is supported by the interaction of BLP with the surface of electronegative GO-PAA-Cu composite to form these activated O-species. These suggestions also proposed by Peng et al. [35], who revealed that magnetic nanometals adsorb proteins such as albumin on their surfaces according to their charge and affinity, influencing their active binding to opposite components. Additionally, Saptarshi et al. [36] established that the production of protein-NP corona is based on several parameters, such as the applied proteins, the medium, and the features of the NPs surface (hydrophobicity and functional groups).

A previous study conducted by El-Fakharany et al. [37] demonstrated that hybrid Cu—Fe nanometals had potent anticancer activity against many treated human cancer cells in vitro through mediating caspase 3-dependent apoptosis action. Also, the combination of LP with a hybrid of Cu—Fe nanometals reduced the proliferation index (ki-67), consequently leading to suppression of Bcl-2 and upregulation of p53 in the treated cancer cells. Interestingly, our results agree with these previously obtained results via a provoking apoptotic mechanism, which is mediated by upregulation of p53 and caspase-9 genes and suppression of Bcl-2 as well as modulate the inflammatory marker of IL-6 in the treated cancer cells. Many previous studies are in agreement with our results, which revealed that BLP mediates its antitumor effect toward the bone cell model via modulation of nuclear factor (NF)-κB [38]— many previous investigations indicated that CuO nanometals had established their antitumor activity on myelogenous leukemia (K562) cell line through down-regulation of tumor genes and reduction of mitochondrial pathways. Significantly [39,40]. The p53 gene is well-known to be one of the most oxidative stress response transcription factors [41]. The upregulation level in the expression of p53 and suppression in the expression of the BAX "Bcl-2 associated X protein"/Bcl-2 ratio enhance the release of cytochrome *c* from the mitochondria and provoke both apoptotic pathway and caspase cascade [42]. Azizi et al. [43] demonstrated that the prepared albumin-coated CuNPs showed their antitumor effect against the MDA-MB-231 cell line via promoting apoptosis route and cell cycle arrest. They revealed that the induction of oxidative stress-mediated this apoptotic mechanism by forming reactive oxygen species. In this work, the capability of adsorbed protein to internalize rapidly by tumor cells owing to the induced permeation and retention effects of protein complexes, that are mediated by the passive permeability of the used protein such as albumin [44].

On the other hand, it can be supposed that the ultimate fate of the conjugated Cu upon uptake by the treated cancer cells will be degrading and generating Cu^{2+} ions. Therefore, after exerting its antitumor effect and being released from the treated cells as ions, they will not have any cytotoxicity against surrounding cells, owing to the safe manner of Cu^{2+} ions at concentrations lower than 500 μM [43].

Regarding particles size determined by particle size distribution intensity (Fig. 6); the finding demonstrated that about 90.3 % of GO-PAA-Cu-LP composite particles were within the size range of 1114 nm and about 9.7 % were existed in average lower than 200 nm. The formed small NPs on the surface of GO were enhanced retention impact and permeation of the prepared GO-PAA-Cu-LP nanocomposite, which is mediated by the passive permeability in the cancer cells, is what allows NPs to be quickly accumulation inside the treated cancer cells. In this context, passive accumulation of the prepared drug in tumor cells owing to the passive permeability and retention impact is considered to be particularly advantageous [45]. The main challenge in using GO for biomedical applications is that it aggregates in solutions high in salts or proteins, such as cell medium and serum, due to electrostatic charge screening and non-specific protein binding on GO. Liu et al. [46] demonstrated that polyethylene glycol (PEG)-functionalized GO nanoscale to load anticancer candidates via noncovalent physisorption and investigated it's in vitro cellular absorption capability. PEGylated nanoscale GO sheets demonstrated substantial tumor uptake and effective photothermal treatment in mice [47]. The uptake of GO-PAA-Cu and GO-PAA-Cu-LP composites by cancer cells might be via an energy-requiring endocytosis process (energy delivered by the 37 °C incubation temperature), which was similar to Liu et al. The modified GO-PAA-Cu-LP is anticipated to enter cells via an effective endocytic process [48,49]. The high cationicity of BLP may enhance cellular uptake of GO-PAA-Cu-LP composite through electrostatic interactions with the negatively charged tumor cell membrane. Hence, the prepared modified GO-PAA-Cu-LP composite can be used as an effective candidate for combating tumors through its ability to kill cancer cells and activate the apoptotic effect against various types of cancer cells.

4. Conclusion

The obtained results in our study showed that combination therapy of the purified BLP with the GO-PAA-Cu composite enhanced their activity against the treated cancer cells. Combination treatment is supposed to be one of the most successful approaches for increasing the efficacy of combined drugs while reducing their dosage. The purified BLP was successfully adsorbed onto the synthesized GO-PAA-Cu composite, forming the GO-PAA-Cu-LP drug conjugate, which was comprehensively examined for its characteristics, in vitro anticancer activity, and apoptotic mechanism. The modified GO-PAA-Cu-LP composite is a well-defined and potent candidate with strong cytotoxicity against different cancer cell lines. The prepared GO-PAA-Cu-LP showed an apoptotic effect by interrupting the cell cycle phases in most checkpoints (sub-G1 and S phases) with downregulating oncogenes and suppressing pro-inflammatory expression in the treated cancer cells. Owing to the potent effect of the modified GO-PAA-Cu-LP in selectively combating different types of tumor cells, we suppose that a dosage reduction will be applied while the lifetime of BLP is prolonged. Before the findings were obtained, the modified GO-PAA-Cu-LP composite was observed as an interesting therapy option for different tumors, and it holds promise for further in vivo studies.

CRediT authorship contribution statement

Abd El Aziz A. Nayl: Writing – review & editing, Writing – original draft, Supervision, Project administration, Funding acquisition, Formal analysis, Conceptualization. **Esmail M. El-Fakharany:** Software, Methodology, Investigation, Formal analysis, Conceptualization. **Ahmed I. Abd-Elhamid:** Software, Methodology, Investigation, Formal analysis, Conceptualization. **Wael A.A. Arafa:** Methodology, Formal analysis, Conceptualization. **Ahmed Hamad Alanazi:** Software, Methodology, Formal analysis. **Ismail M. Ahmed:** Software, Methodology, Formal analysis. **Ashraf A. Aly:** Writing – review & editing, Writing – original draft, Supervision. **Stefan Bräse:** Writing – review & editing, Writing – original draft, Supervision, Funding acquisition.

Declaration of competing interest

This work has not received specific support from any funding agencies in the public, commercial, or not-for-profit sectors and the authors declare that they have no conflict of interest.

Acknowledgment

This work was funded by the Deanship of Graduate Studies and Scientific Research at Jouf University under grant No (DGSSR-2023-02-02109).

The authors acknowledge support from the KIT-Publication Fund of the Karlsruhe Institute of Technology.

Appendix A. Supplementary data

Supplementary data to this article can be found online at https://doi.org/10.1016/j.ijbiomac.2024.138597.

Data availability

No data was used for the research described in the article.

References

[1] A. Fernandez-Fernandez, R. Manchanda, A.J. McGoron, Theranostic applications of nanomaterials in Cancer: drug delivery, image-guided therapy, and multifunctional platforms, Appl. Biochem. Biotechnol. 165 (2021) 1628–1651, https://doi.org/10.1007/s12010-011-9383-z.

[2] A. Sawdon, E. Weydemeyer, C.-A. Peng, Antitumor therapy using nanomaterial-mediated Thermolysis, J. Biomed. Nanotechnol. 10 (2014) 1894–1917, https://doi.org/10.1166/jbn.2014.1917.

[3] X. Sun, Z. Liu, K.W. Welsher, W. Kevin, T.R. Joshua, G. Andrew, Z. Sasa, D. Hongjie, Nano-graphene oxide for cellular imaging and drug delivery, Nano Res. 1 (2008) (2008) 203–212, https://doi.org/10.1007/s12274-008-8021-8.

[4] X. Pei, Z. Zhu, Z. Gan, J. Chen, X. Zhang, X. Cheng, Q. Wan, J. Wang, PEGylated nano-graphene oxide as a nanocarrier for delivering mixed anticancer drugs to improve anticancer activity, Sci. Rep. 10 (2020) 2717, https://doi.org/10.1038/s41598-020-59624-w.

[5] B. Xie, J. Yi, J. Peng, X. Zhang, L. Lei, D. Zhao, Z. Lei, H. Nie, Characterization of synergistic anti-tumor effects of doxorubicin and p53 via graphene oxide-polyethyleneimine nanocarriers, J. Mater. Sci. Technol. 33 (2017) 807–814, https://doi.org/10.1016/j.jmst.2017.05.005.

[6] A. Mallick, A. Nandi, S. Basu, Polyethylenimine coated graphene oxide nanoparticles for targeting mitochondria in cancer cells, ACS Applied Bio Mater. 2 (2018) 14–19, https://doi.org/10.1021/acsabm.8b00519.

[7] M. Pooresmaeil, H. Namazi, β-Cyclodextrin grafted magnetic graphene oxide applicable as cancer drug delivery agent: synthesis and characterization, Mater. Chem. Phys. 218 (2018) 62–69, https://doi.org/10.1016/j.matchemphys.2018.07.022.

[8] A.H.Z. Kalkhoran, S.H. Naghib, O. Vahidi, M. Rahmanian, Synthesis and characterization of graphene-grafted gelatin nanocomposite hydrogels as emerging drug delivery systems, Biomed Phys Eng Express. 4 (2018) 055017, https://doi.org/10.1088/2057-1976/aad745.

[9] N. Ma, J. Liu, W. He, Z. Li, Y. Luan, Y. Song, S. Garg, Folic acid-grafted bovine serum albumin decorated graphene oxide: an efficient drug carrier for targeted cancer therapy, J. Colloid Interface Sci. 490 (2017) 598–607, https://doi.org/10.1016/j.jcis.2016.11.097.

[10] Y. Wan, Z. Lin, Q.G. Zhang, D. Gan, M. Gama, J. Tu, H. Luo, Incorporating graphene oxide into biomimetic nano-microfibrous cellulose scaffolds for enhanced breast cancer cell behavior, Cellulose 27 (2020) 4471–4485, https://doi.org/10.1007/s10570-020-03078-w.

[11] A. Khoshoei, E. Ghasemy, F. Poustchi, M.-A. Shahbazi, R. Maleki, Engineering the pH-sensitivity of the graphene and carbon nanotube based nanomedicines in smart cancer therapy by grafting trimethyl chitosan, Pharm. Res. 37 (2020) 160, https://doi.org/10.1007/s11095-020-02881-1.

[12] M. Abbasian, M.-M. Roudi, F. Mahmoodzadeh, M. Eskandani, M. Jaymand, Chitosan-grafted-poly (methacrylic acid)/graphene oxide nanocomposite as a pH-responsive de novo cancer chemotherapy nanosystem, Int. J. Biol. Macromol. 118 (2018) 1871–1879, https://doi.org/10.1016/j.ijbiomac.2018.07.036.

[13] S. Gooneh-Farahani, S.M. Naghib, M.R. Naimi-Jamal, A critical comparison study on the pH-sensitive nanocomposites based on graphene-grafted chitosan for cancer theragnosis, Multidiscip Cancer Invest. 3 (2019) 5–16, https://doi.org/10.30699/acad pub.mci.3.1.5.

[14] R. Lima-Sousa, D. de Melo-diogo, C.G. Alves, E.C. Costa, P. Ferreira, R.O. Louro, I. J. Correia, Hyaluronic acid functionalized green reduced graphene oxide for targeted cancer photothermal therapy, Carbohydr. Polym. 200 (2018) 93–99, https://doi.org/10.1016/j.carbpol.2018.07.066.

[15] Y. Guo, H. Xu, Y. Li, F. Wu, Y. Li, Y. Bao, X. Yan, Z. Huang, P. Xu, Hyaluronic acid and Arg-Gly-asp peptide modified graphene oxide with dual receptor-targeting function for cancer therapy, J. Biomater. Appl. 32 (2017) 54–65, https://doi.org/10.1177/0885328217712110.

[16] E. Quagliarini, D. Pozzi, F. Cardarelli, G. Caracciolo, The influence of protein corona on graphene oxide: implications for biomedical theranostics, J Nanobiotechnol 21 (2023) 267, https://doi.org/10.1186/s12951-023-02030-x.

[17] T. Yin, J. Liu, Z. Zhao, Y. Zhao, L. Dong, M. Yang, J. Zhou, M. Huo, Redox sensitive hyaluronic acid- decorated graphene oxide for photothermally controlled tumor-cytoplasm-selective rapid drug delivery, Adv. Funct. Mater. 27 (2017) 1604620, https://doi.org/10.1002/adfm.201604620.

[18] E.M. EL-Fakharany, A.I. Abd-Elhamid, N.M. El-Deeb, Preparation and characterization of novel nanocombination of bovine lactoperoxidase with dye decolorizing and anti-bacterial activity, Sci. Rep. 9 (1) (2019) 8530, https://doi.org/10.1038/s41598-019-44961-2.

[19] A.I. Abd-Elhamid, E.M. Abu Elgoud, H.F. Aly, Graphene oxide modified with carboxymethyl cellulose for high adsorption capacities towards Nd(III) and Ce(III) from aqueous solutions, Cellulose 29 (2022) 9831–9846, https://doi.org/10.1007/s10570-022-04862-6.

[20] M.M. Abu-Serie, E.M. El-Fakharany, Efficiency of novel nanocombinations of bovine milk proteins (lactoperoxidase and lactoferrin) for combating different human cancer cell lines, Sci. Rep. 7 (2017) 16769, https://doi.org/10.1038/s41598-017-16962-6.

[21] J.R. Kanwar, K. Roy, Y. Patel, S.-F. Zhou, M.R. Singh, D. Singh, M. Nasir, R. Sehgal, A. Sehgal, R.S. Singh, S. Garg, R.K. Kanwar, Multifunctional iron bound lactoferrin and nanomedicinal approaches to enhance its bioactive functions, Molecules 20 (2015) 9703–9731, https://doi.org/10.3390/molecules20069703.

[22] M.J. Davies, C.L. Hawkins, D.J. Pattison, M.D. Rees, Mammalian heme peroxidases: from molecular mechanisms to health implications, Antioxid. Redox Signal. 10 (7) (2008) 1199–1234, https://doi.org/10.1089/ars.2007.1927.

[23] J. de Wit, A. Van Hooydonk, Structure, functions and applications of lactoperoxidase in natural antimicrobial systems, Neth. Milk Dairy J. 50 (1996) 227–244.

[24] E.M. Redwan, H.A. Almehdar, E.M. El-Fakharany, A.-W.K. Baig, V.N. Uversky, Potential antiviral activities of camel, bovine, and human lactoperoxidases against hepatitis C virus genotype 4, RSC Adv. 5 (2015) 60441–60452, https://doi.org/10.1039/C5RA11768B.

[25] M.M. Cals, P. Mailliart, G. Brignon, P. Anglade, B.R. Dumas, Primary structure of bovine lactoperoxidase, a fourth member of a mammalian heme peroxidase family, Eur. J. Biochem. 198 (1991) 733–739, https://doi.org/10.1111/j.1432-1033.1991.tb16073.x.

[26] S.R. Saptarshi, A. Duschl, A.L. Lopata, Interaction of nanoparticles with proteins: relation to bio-reactivity of the nanoparticle, J. Nanobiotechnology 26 (2013), https://doi.org/10.1186/1477-, 3155-11.

[27] R. Li, Y. Wang, J. Du, X. Wang, A. Duan, R. Gao, J. Liu, B. Li, Graphene oxide loaded with tumor-targeted peptide and anti-cancer drugs for cancer target therapy, Sci. Rep. 11 (2021) 1725.

[28] N.R. Mohamada, N.H.C. Marzukia, N.A. Buanga, F. Huyopb, R. AbdulWahab, An overview of technologies for immobilization of enzymes and surface analysis techniques or immobilized enzymes, Biotechnol. Biotechnol. Equip. 29 (2015) 205–220, https://doi.org/10.1080/13102818.2015.1008192.

[29] H. Nayeri, A. Fattahi, M. Iranpoor-mobarakeh, P. Nori, Stabilization of lactoperoxidase by tragacanth-chitosan nano biopolymer, International Journal of Biosciences 6 (2015) 418–426.

[30] L. Hänström, A. Johansson, J. Carlsson, Lactoperoxidase and thiocyanate protect cultured mammalian cells against hydrogen peroxide toxicity, Med. Biol. 61 (5) (1983) 268–274 (PMID: 6686988).

[31] I.Y. Kim, E. Joachim, H. Choi, K. Kim, Toxicity of silica nanoparticles depends on size, dose, and cell type, Nano medicine: Nanotechnology. Biol Med 11 (2015) 1407–1416, https://doi.org/10.1016/j.nano.2015.03.004.

[32] M. Jaishankar, T. Tseten, N. Anbalagan, B.B. Mathew, K.N. Beeregowda, Toxicity, mechanism and health effects of some heavy metals, Interdiscip. Toxicol. 7 (2014) 60–72, https://doi.org/10.2478/intox-2014-0009.

[33] B. Szachowicz-Petelska, I. Dobrzynska, S. Sulkowski, Z. Figaszewski, Characterization of the cell membrane during cancer transformation, J. Environ. Biol. 31 (5) (2010) 845–885, https://doi.org/10.5772/29559.

[34] B. Halliwell, J.M. Gutteridge, The Chemistry of Free Radicals and Related Reactive Species. Free Radicals in Biology and Medicine, 4th ed., Oxford University Press, Oxford, UK, 2007, pp. 30–78.

[35] Q. Peng, S. Zhang, Q. Qin Yang, T. Zhang, X.-Q. Wei, L. Li Jiang, C.-L. Zhang, Q.-M. Chen, Z.R. Zhang, Y.-F. Lin, Preformed albumin corona, a protective coating for nanoparticles based drug delivery system, Biomaterials 34 (2013) 8521–8530, https://doi.org/10.1016/j.biomaterials.2013.07.102.

[36] S.R. Saptarshi, A. Duschl, A.L. Lopata, Interaction of nanoparticles with proteins: relation to bio-reactivity of the nanoparticle, J Nanobiotechnol 11 (2013) 26, https://doi.org/10.1186/1477-3155-11-26.

[37] F.M. El-Fakharany, M.M. Abu-Serie, N.H. Habashy, M. Eltarahony, Augmenting apoptosis-mediated anticancer activity of lactoperoxidase and lactoferrin by nanocombination with copper and iron hybrid nanometals, Sci. Rep. 12 (2022) 13153, https://doi.org/10.1038/s41598-022-17357-y.

[38] Y. Morita, A.A. Ono, A. Serizawa, K. Yogo, N. Ishida-Kitagawa, T. Takeya, T. Ogawa, Purification and identification of lactoperoxidase in milk basic proteins as an inhibitor of osteoclastogenesis, J. Dairy Sci. 94 (2011) 2270–2279, https://doi.org/10.3168/jds.2010-4039.

[39] M. Shafagh, F. Rahmani, N. Delirezh, CuO nanoparticles induce cytotoxicity and apoptosis in human K562 cancer cell line via mitochondrial pathway, through reactive oxygen species and P53, Iran. J. Basic Med. Sci. 18 (2015) 993. PMID: 26730334; PMCID: PMC4686584.

[40] A. Kalaiarasi, R. Sankar, C. Anusha, K. Saravanan, K. Aarthy, S. Karthic, T. L. Mathuram, V. Ravikumar, Copper oxide nanoparticles induce anticancer activity in A549 lung cancer cells by inhibition of histone deacetylase, Biotechnol. Lett. 40 (2018) 249–256, https://doi.org/10.1007/s10529-017-2463-6.

[41] M. Valko, C.J. Rhodes, J. Moncol, M. Izakovic, M. Mazur, Free radicals, metals and antioxidants in oxidative stress-induced cancer, Chem. Biol. Interact. 160 (2006) 1–40, https://doi.org/10.1016/j.cbi.2005.12.009.

[42] M.A. Siddiqui, H.A. Alhadlaq, J. Ahmad, A.A. Al-Khedhairy, J. Musarrat, M. Ahamed, Copper oxide nanoparticles induced mitochondria mediated apoptosis in human Hepatocarcinoma cells, PloS One 8 (8) (2013) e69534, https://doi.org/10.1371/journal.pone.0069534.

[43] M. Azizi, H. Ghourchian, F. Yazdian, F. Dashtestani, H. AlizadehZeinabad, Cytotoxic effect of albumin coated copper nanoparticle on human breast cancer

cells of MDA-MB 231, PloS One 12 (11) (2017) e0188639, https://doi.org/10.1371/journal.pone.0188639.
[44] F. Bessone, C. Dianzani, M. Argenziano, L. Cangemi, R. Spagnolo, F. Maione, E. Giraudo, R. Cavalli, Albumin nanoformulations as an innovative solution to overcome doxorubicin chemoresistance, Cancer Drug Resist. 4 (1) (2021) 192–207, doi:10.20517/cdr.2020.65. PMID: 35582009; PMCID: PMC9019188 doi: 10.2051.7/cdr.2020.65.
[45] S.K. Hobbs, W.L. Monsky, F. Yuan, W.G. Roberts, L. Griffith, V.P. Torchilin, R. K. Jain, Regulation of transport pathways in tumor vessels: Role of tumor type and microenvironment, Proc. Natl. Acad. Sci. USA. 95 (8) (1998) 4607–4612, doi: 10.1073/pnas.95.8.4607 (1998).
[46] Z. Liu, J.T. Robinson, X.M. Sun, H.J. Dai, PEGylated nanographene oxide for delivery of water-insoluble cancer drugs, J. Americ. Chem. Soc. 130 (2008) 10876–10877.
[47] K. Yang, S.A. Zhang, G.X. Zhang, X.M. Sun, S.T. Lee, Z.A. Liu, Graphene in mice: ultrahigh in vivo tumor uptake and efficient photothermal therapy, Nano Lett. 10 (2010) 3318–3323.
[48] N.W.S. Kam, Z.A. Liu, H.J. Dai, Carbon nanotubes as intracellular transporters for proteins and DNA: an investigation of the uptake mechanism and pathway, Angew. Chemie-Internat. Edit. 45 (2006) 577–581.
[49] T. Kavitha, S.I.H. Abdi, S.-Y. Park, pH-sensitive nanocargo based on smart polymer functionalized graphene oxide for site-specific drug delivery, Phys. Chem. Chem. Phys. 15 (14) (2013) 5176–5185.